energies

MDPI

Article

Performance Enhancement of Hybrid Solid Desiccant Cooling Systems by Integrating Solar Water Collectors in Taiwan

Win-Jet Luo [1,*], Dini Faridah [1], Fikri Rahmat Fasya [2], Yu-Sheng Chen [2], Fikri Hizbul Mulki [2] and Utami Nuri Adilah [3]

1 Graduate Institute of Precision Manufacturing Engineering, National Chin-Yi University of Technology, Zhongshan Rd., Taiping Dist., Taichung 41170, Taiwan
2 Department of Refrigeration, Air Conditioning and Energy Engineering, National Chin-Yi University of Technology, Zhongshan Rd., Taiping Dist., Taichung 41170, Taiwan
3 Department of Refrigeration and Air Conditioning Engineering, Politeknik Negeri Bandung, Gegerkalong Hilir Rd., Parongpong Dist., Bandung 40012, Indonesia
* Correspondence: wjluo@ncut.edu.tw; Tel.: +886-423-924-505 (ext. 5110)

Received: 30 July 2019; Accepted: 4 September 2019; Published: 9 September 2019

Abstract: A hybrid solid desiccant cooling system (SDCS), which combines a solid desiccant system and a vapor compression system, is considered to be an excellent alternative for commercial and residential air conditioning systems. In this study, a solar-assisted hybrid SDCS system was developed in which solar-heated water is used as an additional heat source for the regeneration process, in addition to recovering heat from the condenser of an integrated heat pump. A solar thermal collector sub-system is used to generate solar regeneration water. Experiments were conducted in the typically hot and humid weather of Taichung, Taiwan, from the spring to fall seasons. The experimental results show that the overall performance of the system in terms of power consumption can be enhanced by approximately 10% by integrating a solar-heated water heat exchanger in comparison to the hybrid SDCS system. The results show that the system performs better when the outdoor humidity ratio is large. In addition, regarding the effect of ambient temperature on the coefficient of performance (COP) of the systems, a critical value of outdoor temperature exists. The COP of the systems gradually rises with the increase in ambient temperature. However, when the ambient temperature is greater than the critical value, the COP gradually decreases with the increase in ambient temperature. The critical outdoor temperature of the hybrid SDCS is from 26 °C to 27 °C, and the critical temperature of the solar-assisted hybrid SDCS is from 27 °C to 30 °C.

Keywords: hybrid solid desiccant cooling system; regeneration process; solar thermal collector; coefficient of performance

1. Introduction

Heating, ventilating and air conditioning (HVAC) systems are designed to maintain specific indoor conditions, which vary depending on the application. The main factors that influence the thermal comfort of occupants are metabolic rate, clothing insulation, air temperature, mean radiant temperature, air velocity and relative humidity [1]. The main purpose of the HVAC system is to provide good indoor air quality that meets the criteria for hygienic air conditions and satisfies the thermal comfort of occupants or products in a building or space. Moreover, the working environment can influence the productivity of workers, which is an economic reason for installing HVAC systems in buildings [2,3].

Generally, HVAC systems require a large amount of energy, especially in large capacity applications. HVAC systems make a significant contribution to carbon-based energy consumption and greenhouse gases emissions [4]. In the USA, nearly 50% of the energy consumption of buildings is used for HVAC systems [5]. Furthermore, conventional HVAC systems cause pollution, not only due to consuming a large amount of energy, but also due to the use of hydro-chlorofluorocarbon (HCFC), hydrofluorocarbon (HFC) and other refrigerants that produce greenhouse gases [6].

Cooling-based dehumidification systems are the most popular systems of recent decades [7,8]. Such systems provide cooling and dehumidification by utilizing a single vapor-compression unit. Cooling coils are used to cool the air below its dew point so moisture can be removed from the air. Therefore, low humidity and low temperature air can be generated and a reheat coil is required to avoid overcooling, which consumes a large amount of energy and is difficult to control. Current studies are developing new approaches that are more energy efficient and more environmentally friendly.

Recently, novel modern air conditioning systems have been proposed, most notably utilizing split processes of cooling and dehumidification. Instead of the cooling coil unit used in conventional cooling dehumidification systems, a single unit that can handle latent heat is applied, so unnecessary energy use can be avoided. One developed method is a solid desiccant cooling system (SDCS) in which refrigerants of HCFCs are unnecessary and low-grade thermal energy can be used for regeneration [9,10]. In an SDCS system, solid desiccants, such as silica gel, activated carbon, molecular sieves, alumina gel and other materials with strong hygroscopic ability, are used to dehumidify the process air. The solid desiccant itself has many pores, and the inner surface of each pore is concave. When the process air passes through the solid desiccant, because of the lower partial pressure of water vapor on the concave surface with a small radius of curvature, the vapor may migrate from the air to the concave surface of the pores. Then, the vapor condenses on the concave surface and releases adsorption heat to the desiccant. The most widely used solid desiccant dehumidification equipment is the rotary dehumidification wheel, in which solid desiccant is coated on the surface of wheel. The rotary dehumidification wheel can realize continuous dehumidification and regeneration through periodical rotation. The high-humidity process air passes through a portion of the desiccant wheel, and the vapor in the process air is absorbed by the solid desiccant of the wheel due to the vapor pressure difference between the air and the desiccant. Then, the temperature of the process air rises due to adsorption heat, and humidity is reduced after passing through the wheel. When the desiccant in the process air stream absorbs enough vapor from the process air, the vapor adsorption portion of the desiccant wheel is rotated to the high temperature regeneration air stream. While the regeneration air passes through the portion of the desiccant wheel containing a greater amount of vapor in the desiccant, the heat from the high temperature air stream leads to higher vapor pressure in the desiccant in comparison to the vapor pressure in the air stream. Then, vapor in the desiccant is ejected into the regenerated air stream until the lower vapor pressure condition in the desiccant is attained. The desiccant wheel periodically and dynamically rotates between the process and regeneration air streams. Dehumidification and regeneration processes are conducted in the corresponding air streams, and a low-humidity process air stream can be continuously obtained using the rotary wheel. Narayanan et al. [11] analyzed the performance characteristics of a solid-desiccant evaporative cooling system with TRNSYS software. The results show that the system could provide thermal comfort, however, the capability of the system to provide suitable air temperature and humidity depends on the performance of the evaporative cooling, energy-recovery, and heat-generation systems. Therefore, the availability of a cheap or waste-heat source is essential in making this system economically viable. Narayanan et al. [12] numerically investigated the dehumidification potential of a solid desiccant-based evaporative cooling system with an enthalpy exchanger operating in subtropical and tropical climates with TRNSYS software. The results show that in hot and humid conditions, the system thermal comfort capability drops to around 54% to 63%.

Solar energy utilization is a new approach developed in recent years specifically for space heating applications. The solar energy source is limitless and safer for the environment. Recently, heat from

solar energy was developed for desiccant cooling systems. The heat generated by a solar thermal collector can be used for the regeneration process of the dehumidification wheel. Guidara et al. [13] proposed the use of evaporative coolers for pre-cooling and re-cooling of the process air before and after the dehumidification wheel in order to satisfy the load demand of an air-conditioned space. From their numerical analysis, they indicated that the pre-cooling design is suitable to be applied in drier ambient conditions. Enteria et al. [14] investigated the performance of a solar-desiccant cooling system with a silica gel and titanium dioxide desiccant wheel in East Asia. From numerical simulations, it was found that using solar desiccant cooling systems has great potential for East Asian countries. The study pointed out that, in the tropical region, a larger area and capacity of the solar thermal collector and greater regeneration air flow rate are required, and the operational performance of the system is in the range of 1.5 to 3. The major operational energy loss of the proposed system comes from solar collectors, water pipes, electric heaters and thermal storage tanks. Speerforck et al. [15] numerically investigated the performance of a solar-desiccant cooling system incorporating borehole heat exchangers for direct cooling and solar energy for desiccant regeneration. They indicated that the proposed system allows electricity saving of 50% and reduces CO_2 equivalent emissions by 91%. White et al. [16] proposed a solar-assisted SDCS incorporating direct and indirect evaporative coolers in a serial arrangement to cool process air after the dehumidification wheel. From numerical analysis, it was indicated that the sensible heat removal capability of the process air can be enhanced by a two-stage evaporative cooling design, which is suitable for cities with low-humidity climatic conditions.

Environmental conditions in different regions may affect the performance of a desiccant cooling system (DCS). In hot and humid regions, the use of a hybrid SDCS that is integrated with a heat pump is suggested, instead of a conventional SDCS that utilizes an evaporative cooler and can generate a more humid air supply. Jani et al. [17] proposed a hybrid cooling system integrated with a heat pump (hybrid SDCS), and indicated the proposed system has good performance in hot and humid climate conditions. The dehumidification performance of the system is also highly sensitive to the outdoor ambient conditions. The performance of the hybrid SDCS is better for cases where ambient humidity is high [18]. It was found that the use of a hybrid SDCS can decrease the total power consumption by 20–30% and increase the cooling capacity by 40–60% [19]. Jani et al. [20] used the numerical software TRNSYS to simulate the performance of a solid desiccant-assisted hybrid space cooling system. The results show that the system achieves a good performance in hot humid climates. The humidity ratio of a room's process air was substantially lowered, from 0.014 kg of water/kg of dry air to 0.006 kg of water/kg of dry air, by use of a solid desiccant-based rotary dehumidifier.

In addition to environmental conditions, regeneration temperature is one of the main parameters used to determine the performance of a SDCS. The performance of an SDCS is sensitive to changes in humidity and regeneration temperature [21,22]. However, if the regeneration temperature in the hybrid SDCS is too high, the system performance may be reduced due to high condensation pressure and an increased amount of work performed by the compressor. Several heat sources can be used for the regeneration process, such as an electric heater, gas, a low-grade thermal energy such as solar energy, and waste heat. A further cogeneration system can also be considered as the heat source for the regeneration process.

Beccali [23,24] developed a new solar-assisted hybrid SDCS in which the condensing heat from the condenser of the incorporated heat pump is recovered to preheat the regeneration air stream before solar heating. Long-term measurements of the developed system were conducted in southern Italy. Five control modes based on the temperature and humidity of the outdoor air conditions were designed. From their performance analysis, it was pointed out that preheating of the recovered heat for the regeneration process can reduce the required heat from the solar collector by approximately 30%. In other words, the required area of the solar collector can also be moderately reduced. Fong et al. [25,26] developed a solar-assisted SDCS incorporating an adsorption chiller and analyzed the performance of the system by numerical analysis. The outdoor air was dehumidified by a rotary dehumidification wheel and passed through a radiant cooling coil in an air-conditioned space. The chilled water from

the adsorption chiller was provided to the radiant cooling coil for handling the sensible heat of the air-conditioned space. Both required regeneration heating for the rotary dehumidification wheel and the adsorption chiller supplied by the solar collector. Compared with the traditional centralized air conditioning system, the energy saving potential of the integrated system could reach 36.5%. As alternatives to silica gel, Bareschino et al. [27] proposed other hygroscopic materials for desiccant wheels, MIL101@GO-6 (MILGO) and Campanian ignimbrite, in conjunction with an air-conditioning system driven by evacuated tube solar collectors equipped with a desiccant wheel. The numerical simulations were carried out by means of TRNSYS 17® (version 17, Thermal Energy System Specialists, Madison, WI, USA) to dynamically assess the energy flows in the considered plants and compared with that of a conventional system. The results demonstrate that primary energy savings of approximately 20%, 29%, and 15% can be reached with silica-gel, MILGO and zeolite-rich tuff desiccant wheel-based air handling units, respectively. Li et al. [28] investigated a two-stage rotary desiccant cooling/heating system driven by evacuated glass tube solar air collectors. The results show that the major advantage of the two-stage desiccant cooling system was that moisture removal reached 6.68–14.43 g/kg in hot and humid climate conditions. Solar heating with desiccant humidification can improve indoor comfort significantly. A solar hybrid SDCS is a good substitute for traditional vapor compression air conditioning systems, especially in hot and humid climates, since solar energy can result in energy savings in the range of 40–45% [29]. Rambhad [30] indicated regeneration temperatures of hot water in the range of 54.3 °C to 68.3 °C can be achieved in solar SDCS systems by simulation.

In previous studies, the solar-assisted hybrid SDCS system was considered a replacement of the refrigerant vapor compression air conditioning system due to its higher energy efficiency. However, most studies of the solar-assisted hybrid SDCS have been conducted using numerical analysis. Research into the system's long-term practical operations and analysis of its performance under the effects of different ambient temperatures and humidity ratios is less common, especially in hot and humid environments. The performance of the solar-assisted hybrid SDCS has not been investigated experimentally in detail. In this study, the effect of ambient humidity and temperature on the performance of a solar-assisted hybrid SDCS was investigated under the high humidity and high temperature ambient conditions of Taichung, Taiwan. The performance analysis and comparisons of solar-assisted hybrid SDCS, hybrid SDCS and solar SDCS systems were conducted through long-term experiments in order to understand their characteristics and operational ranges in terms of environmental conditions.

2. Experimental Configuration and Methods

The experiments were conducted in the typical hot and humid weather of Taichung. The city has four seasons with an average temperature of 23.3 °C. The monthly average temperature, average relative humidity (*RH*) and the solar irradiation of Taichung from April to October are listed in Table 1. In the solar hybrid SDCS system, the heat from solar collectors and the condenser of an integrated heat pump sub-system are used for regeneration.

Table 1. Monthly average temperature, relative humidity (*RH*) and solar irradiation of Taichung [31].

Month	Temperature (°C)	*RH* (%)	Solar Irradiation (W/m^2)
April	27.6	77.3	154.142
May	30.2	77.1	162.474
June	31.9	77.9	166.640
July	33.0	75.6	174.972
August	32.6	77.6	164.557
September	31.8	75.8	162.474
October	30.1	72.6	158.308

2.1. Proposed System Configuration

In general, the proposed solar-assisted hybrid SDCS is divided into two major sub-systems. The first is a hybrid SDCS and the second is a solar-heated water system. The solar collector is installed at a fixed tilt angle of 27° facing the south-east direction. Several configurations, including a hybrid SDCS system, solar-assisted SDCS systems and a solar-assisted hybrid SDCS system, were studied to investigate the effect of using a solar regeneration water system on system performance.

2.1.1. Hybrid SDCS Configuration

The hybrid SDCS configuration was the first configuration investigated. In this configuration, the only heat source for the regeneration process is the condenser of the integrated heat pump, as shown in Figure 1. In this configuration, chilled water is generated by the evaporator and stored in a chilled water tank. The chilled water is pumped to pre-cooling and cooling coils in order to cool process air from the environment. In the integrated heat pump sub-system, an additional condenser installed outside the air handling unit can eject excessive condensation heat to the surroundings and avoid the over-loading of the compressor due to higher condensation temperature in the refrigeration cycle. The return air stream gains heat from the condenser inside the air handling unit, then heats the upper part of the solid desiccant wheel and causes the vapor pressure in the solid desiccant to be higher than the vapor pressure in the air stream. The moisture in the solid desiccant is ejected to the surroundings with the air stream. The moisture removal from the desiccant wheel by additional heat in the return air stream is called the regeneration process.

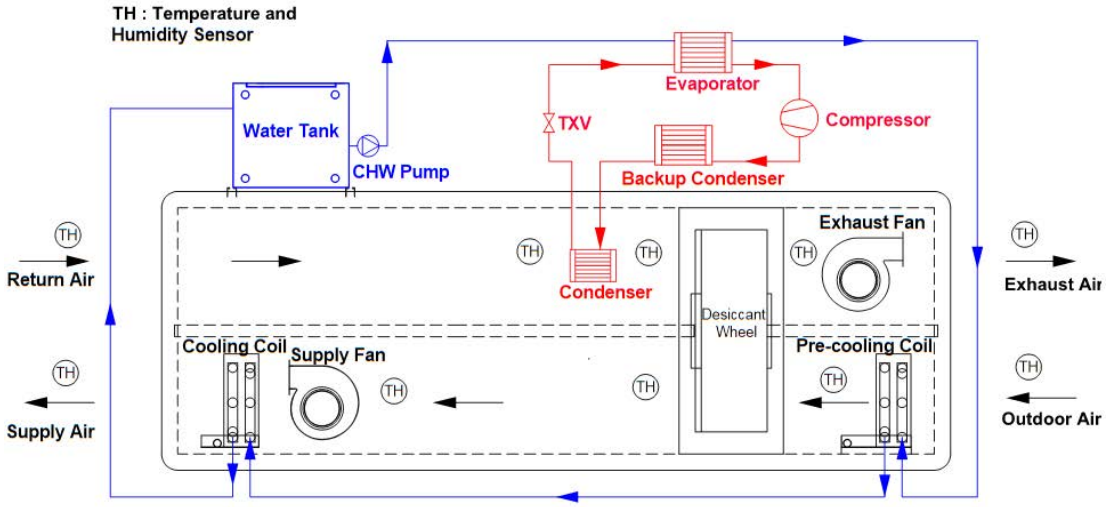

Figure 1. Hybrid solid desiccant cooling system (SDCS) configuration.

2.1.2. Solar-Assisted SDCS Configuration

The solar-assisted SDCS configuration is shown in Figure 2. The configuration only uses solar-heated water from a heat exchanger as the heat source for regeneration. Therefore, the regeneration temperature of the system will not be as high as the regeneration temperature of the hybrid SDCS configuration. In terms of process air, latent heat is handled by the desiccant wheel. However, since the heat pump is turned off, the temperature gradually increases with operation time due to adsorption heat in the dehumidification process. Therefore, the supply air temperature will be higher compared to other cases.

2.1.3. Solar-Assisted Hybrid SDCS Configuration

In the solar-assisted hybrid SDCS configuration, the condensing heat of the integrated heat pump and the heat of solar-heated water are used as heat sources for the regeneration process. In the

regeneration air stream, the returning air is pre-heated by solar-heated water from a heat exchanger. Then, the returning air passes the condenser of the integrated heat pump to recover the dissipating heat from the condenser again in order to increase the regeneration temperature. In terms of process air, the air handling process concept is the same as in the hybrid SDCS configuration. The corresponding system configuration is shown in Figure 3.

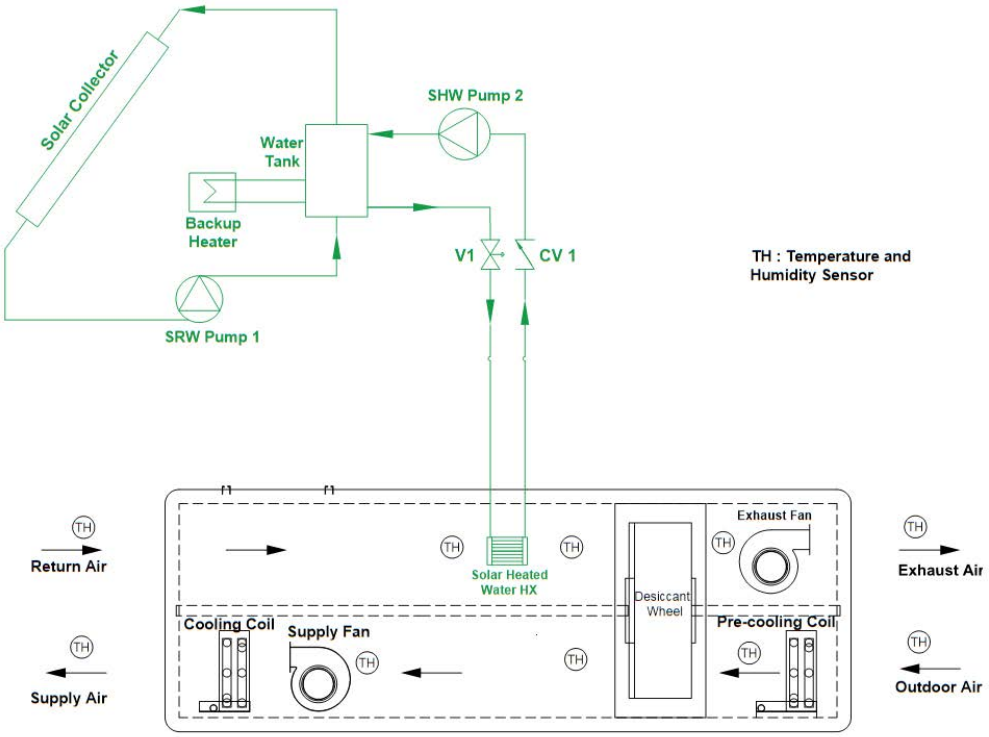

Figure 2. Solar-assisted SDCS configuration.

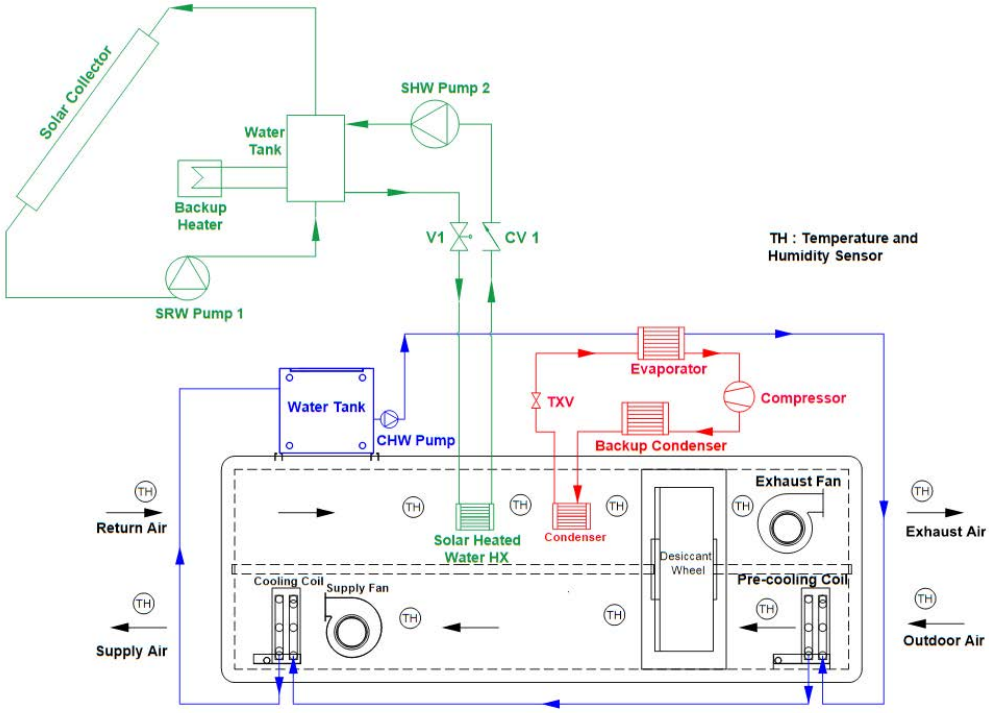

Figure 3. Solar-assisted hybrid SDCS configuration.

The system specifications are as follows:

(1) Desiccant wheel: rotor depth 0.2 m, diameter 0.3 m, rotational speed 10 rph, thermal effectiveness 75%; silica gel, ProFlute (Stockholm, Sweden).
(2) Compressor: capacity 6 kW, 220 volts (V)/7.3 amperes (A), locked rotor ampere (LRA), frequency 60 Hertz (Hz); R407c refrigerant, Tecumseh (Ann Arbor, MI, USA).
(3) Condenser: finned and tube condenser, 730 × 290 × 200 mm (main condenser), 530 × 290 × 100 mm (auxiliary condenser).
(4) Supply and exhaust fans: nominal power 0.7 kW, frequency 0–50 Hz.
(5) Cooling water tank: capacity 71 L.
(6) Chilled-water pump: nominal capacity 0.37 kW, rotational speed 3370 rpm, 220 V/1.5 A, flow rate 25 m^3/h, chilled water temperature: 13 °C.
(7) Solar thermal collector (Sun Tech, Taichung, Taiwan): number of tubes 18, effective area 1.974 m^2, total gross area 11.699 m^2, effectiveness 94.5%.
(8) Solar water tank: capacity 100 L.
(9) Solar-heated water heat exchanger: finned and tube HX, 400 × 360 × 200 mm.
(10) Temperature and relative humidity (*RH*) sensors: ECOA EPRTH04101 (Ecoa Technologies, Taipei, Taiwan), 0–100 °C, 0–100% *RH*, temperature measurement accuracy ±0.3 °C at 25 °C, *RH* measurement accuracy ±4% *RH* (at 10–90%) and ±6% *RH* (at 0–10% and 90–100%).
(11) Current sensors: CTT-CLS-CV clamp on type (U.R.D., Yokohama, Japan), current range 0–100 A, measurement accuracy ±2%.
(12) Flow meter sensor: TESTO480 hot wire anemometer (Testo, West Chester, PA, USA), velocity measurement accuracy ±0.21 at 1.96 m/s, ±0.29 at 4.99 m/s, and ±0.41 at 10.06 m/s.

In terms of air flow rates, the flow rates of the process air and regeneration airstreams are not the same due to a slight leakage in the system. However, the gap between the two flow rates is small. The flow rate of the process stream is 465 m^3/hour, while the flow rate of the regeneration stream is 400 m^3/hour. The flow rates of both air streams are obtained by adjusting the frequency of the fans. In addition, the flow rate of the solar-heated water heat exchanger is 40 L/min. The thermal effectiveness of the solar-heated water heat exchanger is 62.03%.

2.2. Theoretical Analysis

The system's performance is analysed using theoretical analysis. The coefficient of performance, COP_{hvac} in Equation (1) is the ratio of the total cooling capacity, Q_c (kW), to the total power consumption of the system, E_{tot} (kW):

$$COP_{hvac} = Q_c/E_{tot} \quad (1)$$

The total cooling capacity of the system, Q_c (kW), is calculated by Equation (2):

$$Q_c = \dot{m}_p\,(h_{oa} - h_{sa}) \quad (2)$$

where h_{oa} (kJ/kg) is the specific enthalpy of outdoor air and h_{sa} (kJ/kg) is the specific enthalpy of supply air. The total power consumption in Equation (3) consists of the fan power, P_{fan} (kW), compressor power, P_{comp} (kW), water pump power, P_{pump} (kW) and other electrical components, P_{other} (kW):

$$E_{tot} = P_{fan} + P_{comp} + P_{pump} + P_{other} \quad (3)$$

In the supply air stream, the latent heat performance, COP_{lt}, of the system in Equation (4) is the ratio of latent heat capacity, Q_{lt} (kW), to the total power consumption of the system:

$$COP_{lt} = Q_{lt}/E_{tot} \quad (4)$$

The latent heat capacity, Q_{lt} (kW), of the system is calculated by Equation (5):

$$Q_{lt} = \dot{m}_p \, (h_{oa} - h') \tag{5}$$

where h' (kJ/kg) is the specific enthalpy of air with the temperature of the outside air and the humidity ratio of the supply air.

The specific moisture removal, SMR (kg/kg$_{da}$), is the humidity ratio difference between the outdoor air, ω_{oa} (kg/kg$_{da}$), and the supply air, ω_{sa} (kg/kg$_{da}$), along the process air stream. The SMR value can be calculated by Equation (6):

$$SMR = \omega_{oa} - \omega_{sa} \tag{6}$$

The effectiveness of the desiccant wheel, ε, is defined by Equation (7):

$$\varepsilon = SMR/(\omega_{oa} - \omega_i) \tag{7}$$

where the ideal specific moisture, ω_i, is assumed to be 0 kg/kg$_{da}$; thus, the denominator is the maximum moisture that can be removed by the desiccant wheel system. The moisture removal rate, MRR (kg/h), can be calculated by Equation (8):

$$MRR = \dot{m}_p \, (\omega_{oa} - \omega_{sa}) \, 3600 \tag{8}$$

where $\dot{m}_p$ is the mass flow rate of the process air stream (kg/s). The solar fraction, SF, is determined by Equation (9):

$$SF = E_{sol}/E_{tot.m} \tag{9}$$

where E_{sol} (MJ) is the total useful solar thermal energy available in a month, which can be obtained from the solar collector capacity Q_{sol} (kW). Q_{sol} (kW) can be calculated by Equation (10).

$$Q_{sol} = \eta_{soc} \, A_{soc} \, R \tag{10}$$

where η_{soc} is the solar thermal collector overall efficiency, A_{soc} (m^2) is the gross area of the solar thermal collector, and R (kW/m^2) is the total incident solar radiation. In this study, the efficiency, η_{soc}, and the total area, A_{soc}, of the solar thermal collector are 94.5% and 11.699 m^2, respectively. The total energy input in a month, $E_{tot.m}$ (MJ), can be obtain from the total power P_{tot} (kW). P_{tot} (kW) can be calculated by Equation (11):

$$P_{tot} = I_{tot} \, V \tag{11}$$

where I_{tot} and V are the total current and voltage of the system, respectively.

3. Results and Discussion

3.1. Comparison of Average Temperature Declination and Specific Moisture Removal

A comparison of the temperature declination (T_d) and SMR of each system in different months in 2018 is shown in Table 2, where T_d is the temperature drop between the average outdoor air temperature (T_{oa}) and the average supply air temperature (T_{sa}).

According to the table, the temperature declination of the hybrid SDCS and solar-assisted hybrid SDCS are almost the same, while the solar-assisted SDCS does not have a cooling effect because the heat pump is turned off. The cooling and moisture removal of the process air by the solar-assisted hybrid SDCS are the highest among the three configurations. It can be seen that, for the solar-assisted SDCS, the average temperature declination is in the range of 3.65 °C to 6.79 °C, which gradually increases from April to June and then gradually decreases until October. Regarding moisture removal,

the average *SMR* value is in the range of 0.0033 kg/kg$_{da}$ to 0.0075 kg/kg$_{da}$, which also gradually rises from April to June then declines until October.

Table 2. Comparison of T_d and specific moisture removal (*SMR*) for different system configurations.

Month	Average T_{oa}	Average W_{oa}	Hybrid SDCS		Solar-Assisted SDCS		Solar-assisted Hybrid SDCS	
			T_d (°C)	*SMR* (kg/kg$_{da}$)	T_d (°C)	*SMR* (kg/kg$_{da}$)	T_d (°C)	*SMR* (kg/kg$_{da}$)
April	24.75	0.0136	5.21	0.0037	N/A	0.0015	5.35	0.0043
May	28.36	0.0153	5.62	0.0041	N/A	0.0014	5.71	0.0054
June	28.27	0.0163	5.04	0.0061	N/A	0.0013	5.66	0.0055
July	29.93	0.0183	6.42	0.0066	N/A	0.0028	6.79	0.0075
August	27.06	0.0177	3.65	0.0052	N/A	0.0012	3.69	0.0053
September	28.26	0.0176	3.50	0.0040	N/A	0.0011	3.65	0.0046
October	24.65	0.0133	5.18	0.0031	N/A	0.0011	5.23	0.0033

3.2. Comparison of Regeneration Temperatures for Each System Configurations

A comparison of the regeneration temperature of each system during one day is shown in Figure 4. The regeneration temperature samples shown are for the system operating in better ambient conditions with enough sunlight intensity. As shown in Figure 4, the peak regeneration temperature value is generally reached between 14:00 and 16:00 each day. The regeneration temperature of each system is affected by the ambient temperature, especially for the solar-assisted SDCS and solar-assisted hybrid SDCS, in which the heat of solar-heated water is used as an additional heat source.

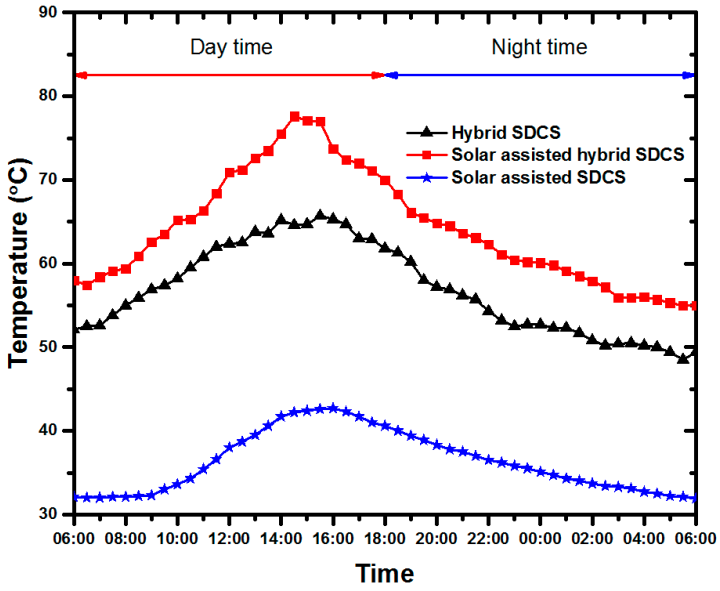

Figure 4. Comparison of regeneration temperature in each system configuration.

It can be observed from Figure 4 that, for a given time, the regeneration temperature of the solar-assisted hybrid SDCS is the highest among the three configurations; the temperature gradually rises from 57 °C at 06:00 to a peak value of 79 °C at 14:00, then gradually decreases to a lowest value of about 55 °C. In the case of the hybrid SDCS, the regeneration temperature distribution is similar to that of the solar-assisted hybrid SDCS, which is in a range of 49 °C to 65 °C. A peak value of 65 °C is attained at about 16:00. In the case of the solar-assisted SDCS, the regeneration temperature is in a range of 32 °C to 43 °C, and the peak value of 43 °C is attained at 16:00. These tendencies also occurred

on other days. In general, the peak regeneration temperature is reached in the time range from 14:00 to 16:00.

Solar fraction (*SF*) is an important technical indicator to assess the feasibility of solar cooling systems. The higher the value of *SF*, the greater the contribution of solar energy to the system. *SF* is the ratio of the solar energy contribution to the total energy input needed to drive the solar cooling system. The total useful solar energy was described in the previous section and the total energy input of the system is the total energy input for the system's operation per month. The average *SF* value of the solar-assisted hybrid SDCS for each month is provided in Figure 5. As shown in Figure 5, it can be observed that the solar collector system shows a high contribution in July. This is because it is the peak summer season at this time, so the energy gained from the solar system is higher. On the other hand, the total energy required to operate the system is approximately constant in each month. The *SF* of the system in July is 0.82 and the lowest *SF* occurs in March with the value of 0.673.

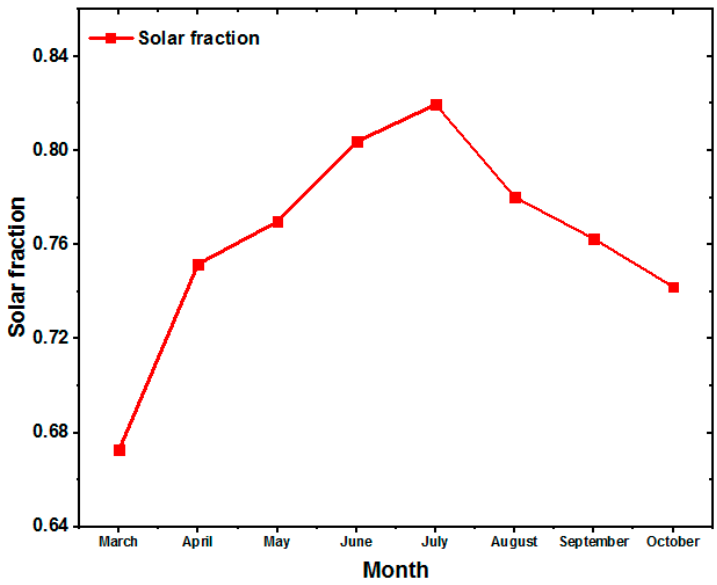

Figure 5. Solar fraction (*SF*) of solar-assisted hybrid SDCS.

3.3. Comparison of Specific Moisture Removal and Moisture Removal Rate

The effect of increasing relative humidity (*RH*) on *SMR* for each configuration is shown in Figure 6, where the outdoor air temperatures are 26 °C, 28 °C and 30 °C, respectively. However, the maximum *RH* attained by the three configurations at 28 °C and 30 °C is only 80% due to the effect of the ambient temperature of the seasons during the experiments. For a constant temperature, the value of relative humidity, *RH* (%), determines the humidity and specific vapor pressure of the process air. At the same process air temperature, higher *RH* values result in higher humidity ratios and vapor pressure. The higher vapor pressure value results in higher pressure differences between the process air and solid desiccant material, which can enhance the adsorption effect of the desiccant material. Thus, the *SMR* value of each configuration tends to increase with the increase in the *RH* value. At the same relative humidity value, the higher humidity ratio of the process air with higher temperature leads to a higher vapor pressure of the process air; thus, the *SMR* value of each configuration is also better for the higher outdoor temperature of 30 °C, as shown in Figure 6. In the solar-assisted SDCS, the *SMR* of the system is relatively low. The system only has a dehumidification effect if the *RH* value is greater than 65%. The *SMR* value of the configuration at an outdoor temperature of 26 °C and 85% *RH* is 0.00262 kg/kg$_{da}$.

The *SMR* of the hybrid SDCS is greater than the solar-assisted SDCS for any *RH* value, with the highest value of 0.0048 kg/kg$_{da}$ at an outdoor temperature of 26 °C and 85% *RH*. The *SMR* of the solar-assisted hybrid SDCS is the largest under all relative humidity conditions, with a maximum value of 0.0063 kg/kg$_{da}$ under the same operational conditions. The reason for this phenomena is

that the solar-assisted hybrid SDCS has the highest regeneration temperature, which can enhance the adsorption effect of the desiccant material.

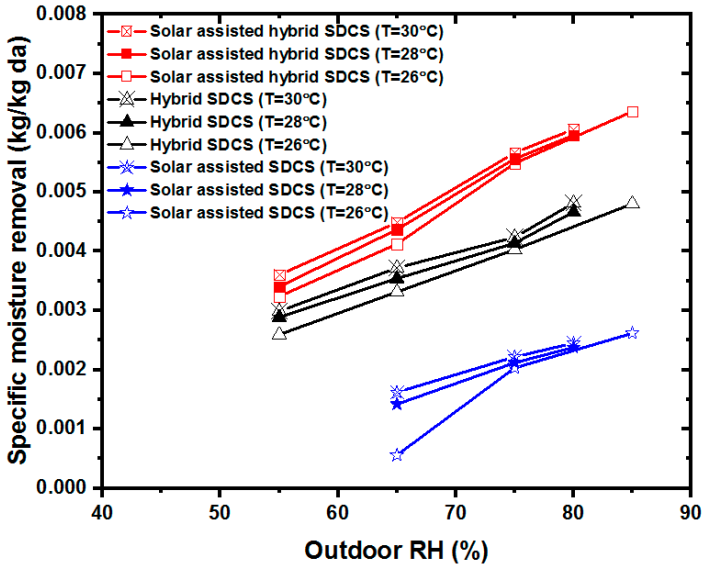

Figure 6. Effect of outdoor relative humidity (*RH*) on *SMR*.

Regarding the humidity ratio effect on *MRR* for each configuration, Figure 7 shows the distributions of moisture removal rate (*MRR*) of the three configurations with the increase in the humidity ratio at an outdoor operational temperature of 26 °C. However, the humidity ratio range of the solar-assisted SDCS and hybrid SDCS is narrower than the humidity ratio range of the solar-assisted hybrid SDCS due to the weather conditions during the experiments. As shown in Figure 7, larger humidity ratios lead to better *MRR* values. The solar-assisted SDCS has the lowest *MRR* value due to lower regeneration temperature. The *MRR* value of the hybrid SDCS and solar-assisted hybrid SDCS is better in comparison to the solar-assisted SDCS configuration. This indicates the regeneration temperature of both systems is sufficient to reactivate the desiccant material. Thus, the *MRR* values of the two configurations are also larger. When the humidity ratio of outdoor air reaches 0.018 kg/kg$_{da}$, the *MRR* can attain to a high value of 3.5 kg/h in the case of the solar-assisted hybrid SDCS.

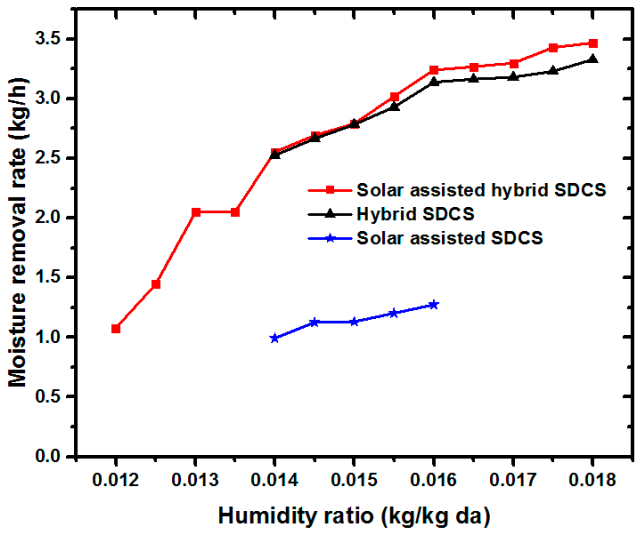

Figure 7. Effect of outdoor humidity ratio on moisture removal rate (*MRR*).

3.4. Effect of Relative Humidity to Desiccant Wheel Effectiveness

The specific moisture removal (*SMR*) value of a solid desiccant configuration determines the moisture removal capability of the system. It can represent the vapor mass of process air absorbed by the solid desiccant material to be ejected to the surroundings. The moisture removal effectiveness of solid desiccant is also determined by the *SMR* value. On the other hand, the *SMR* value is mostly affected by the relative humidity of the outdoor air. The effect of the relative humidity of outdoor air on solid desiccant effectiveness at constant air temperatures of 26 °C and 28 °C is shown in Figure 8. As shown in Figure 8, the effectiveness of solid desiccant increases with the rise in outdoor air relative humidity. At the outdoor temperature of 26 °C and outdoor relative humidity of 50%, the desiccant effectiveness is 0.274, and this value continues to increase as relative humidity increases. The effectiveness value at a relative humidity of 85% is 0.36. The increase in the relative humidity value at the same outdoor air temperature leads the humidity ratio of outdoor air, ω_{oa}, rises, together with the *SMR* value. In the case of this study, the solar-assisted hybrid SDCS increment value of *SMR* in all configurations is greater than the increment of the humidity ratio of outdoor air. Thus, from the definition of desiccant effectiveness, the effectiveness value gradually increases with the increase in relative humidity at the same outdoor air temperature. However, at the same relative humidity value, the effectiveness of solid desiccant wheel in the case with higher process air temperature is less than that with lower process air temperature. The effectiveness of the desiccant wheel is the ideal specific moisture, ω_i, which is assumed to be 0 kg/kg$_{da}$, so the denominator is the maximum moisture that can be removed by the desiccant wheel system. Increasing outdoor temperature with the same relative humidity causes the process air to have a higher humidity ratio. However, with the increase in outdoor air temperature, the increase in the *SMR* value is lower relative to the ideal moisture able to be removed by the system. Therefore, the effectiveness decreases with the temperature of the process air at the same relative humidity ratio.

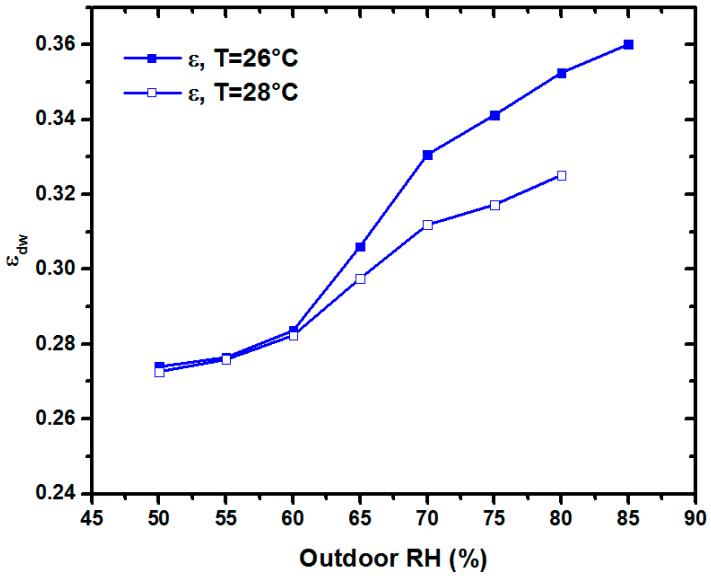

Figure 8. Effect of outdoor *RH* on desiccant effectiveness.

3.5. Effect of Regeneration Temperature to Specific Moisture Removal and Latent Heat Performance

It was mentioned in the previous section that the regeneration temperature impacts the moisture removal ability of the SDCS. The effect of regeneration temperature on specific moisture removal (*SMR*) of the SDCS is shown in Figure 9. The present investigation shows the regeneration temperature effect of each system. The regeneration temperature of the solar-assisted SDCS is in the range of 35–45 °C, while the regeneration temperature of the hybrid SDCS ranges from 50 to 65 °C and the

regeneration temperature of the solar-assisted hybrid SDCS ranges from 55 to 70 °C. The regeneration temperatures can then be drawn as a single line as shown in Figure 9. The effect of regeneration temperature on specific moisture removal and COP_{lt} are thus investigated in this section. In addition to ambient temperature, the regeneration temperature also depends mostly on the capacity of the heat source. In Figure 9, the results are shown for a relative humidity ratio range of 58–62%. As shown in Figure 9, it can be concluded that a higher regeneration temperature leads to a higher *SMR* value. Consequently, the supply air condition will also be drier. If the regeneration temperature is in the range of 35–45 °C, the *SMR* is less than 0.002 kg/kg_{da}, which is not sufficient for the supply air condition. The average regeneration temperature of the solar-assisted SDCS in this study is about 40.4 °C. Even the dehumidification effect will not be apparent if the regeneration temperature is less than 35 °C. However, for the hybrid SDCS, the average regeneration temperature is about 53.9 °C. The higher average regeneration temperature of the hybrid SDCS provides a better *SMR* value than the solar-assisted SDCS. In addiition, the solar-assisted hybrid SDCS possesses the highest regeneration temperature, with an average value of 63.7 °C. Therefore, the *SMR* value of the solar-assisted hybrid SDCS is higher and the dehumidification performance is better among the three configurations.

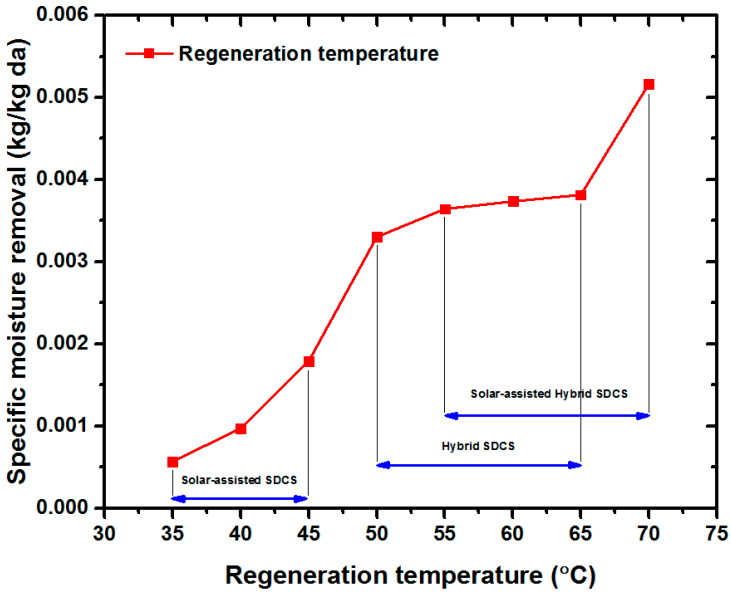

Figure 9. Effect of regeneration temperature on *SMR*.

The effect of regeneration temperature on latent heat performance (COP_{lt}) can be observed in Figure 10. In this case, the outside air relative humidity (*RH*) is also in the range of 58–62%. It can be seen that the COP_{lt} value increases as the regeneration temperature rises from 35 °C to 70 °C. The regeneration temperature depends on the heat generated by heat sources. In the solar-assisted SDCS with the regeneration temperature range of 30 °C to 45 °C, the COP_{lt} of the system is comparatively low. Therefore, the dehumidification effect is also low. The COP_{lt} of the system at a regeneration temperature of 45 °C is 0.556.

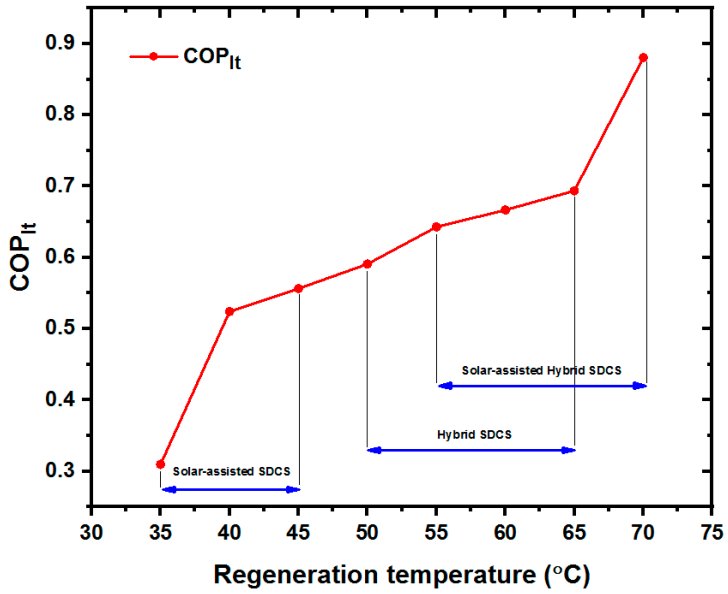

Figure 10. Effect of regeneration temperature on latent heat performance (COP_{lt}).

In the hybrid SDCS, in which the regeneration temperature is in the range of 50 °C to 65 °C, the dehumidification performance is better in comparison to the previous case. The increase in regeneration temperature shows a performance improvement in the system. The COP_{lt} of the hybrid SDCS under an average regeneration temperature of 55 °C is 0.643. The COP_{lt} value shows a massive inclination in the range from 55 °C to 70 °C. It indicates that the optimum regeneration temperature of the desiccant cooling system is 70 °C or higher. However, in this case, the maximum temperature that can be generated by the system is 70 °C. This condition occurs while the system utilizes the solar-assisted hybrid SDCS. The heat from the solar water heat exchanger can effectively increase the regeneration temperature of the system. The COP_{lt} of the solar-assisted hybrid SDCS at the average regeneration temperature of 65 °C is 0.694 and at the maximum regeneration temperature 70 °C is 0.88.

3.6. Comparison of System Total Performance for Different Outdoor Air Temperatures

Figure 11 shows a comparison of COP_{hvac} for each configuration at different outdoor temperatures.

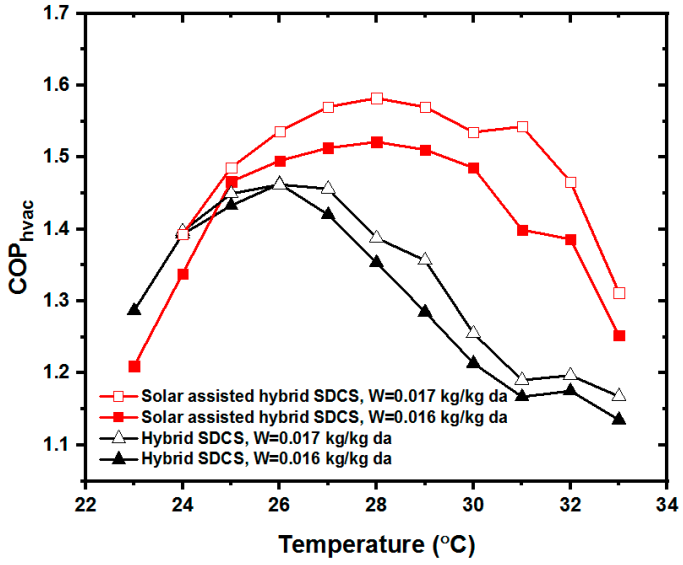

Figure 11. Comparison of the coefficient of performance (COP_{hvac}) at different outdoor temperatures.

The humidity ratio is maintained at 0.016 kg/kg$_{da}$ and 0.017 kg/kg$_{da}$. However, the COP_{hvac} of the solar-assisted SDCS is not investigated since it does not have a cooling effect. Figure 11 indicates the COP_{hvac} is greater for the solar-assisted hybrid SDCS than for the hybrid SDCS, especially at high outdoor temperatures. At low outdoor temperatures, the solar sub-system does not have a significant effect on the system, since the heat from solar-heated water and the regeneration temperature are smaller. At outdoor temperatures from 26 to 30 °C, the performance enhancement of the solar-assisted hybrid SDCS is obvious. At a humidity ratio of 0.016 kg/kg$_{da}$, the maximum COP_{hvac} of 1.52 can be reached by the solar-assisted hybrid SDCS at an outdoor temperature of 28 °C, and the maximum COP_{hvac} of 1.58 can be reached by the system at an outdoor humidity of 0.017 kg/kg$_{da}$.

The solar-assisted hybrid SDCS has better performance at high outdoor temperatures than the hybrid SDCS. However, if the outdoor temperature is too high, system performance is degraded because the condensation temperature rises with the increase in outdoor temperature, which leads to an increase in the power consumption of the compressor. The maximum outdoor temperature in the solar-assisted hybrid SDCS is 30 °C, and in the hybrid SDCS is 26 °C.

3.7. Comparison of System Total Performance for Different Outdoor Humidity

Figure 12 shows a comparison of COP_{hvac} for each system configuration at different outdoor humidities. The outdoor air temperatures in this figure are 26 °C and 32 °C, respectively. The COP_{hvac} of the configuration at an outdoor temperature of 32 °C and humidity less than 0.013 kg/kg$_{da}$ are not provided due to operational environment limitations. The result shows an increase in the outdoor humidity leads to better system performance. The COP_{hvac} inclination of solar assisted SDCS in every 1 g/kg$_{da}$ humidity ratio is about 6.17%, which is higher than that of the hybrid SDCS with the vaue of 5.4%. The COP_{hvac} of the solar-assisted hybrid SDCS is approximately 3.7% greater than that of the hybrid SDCS. The reason for this is that the solar-assisted hybrid SDCS has better *MRR* and dehumidification effects. The maximum COP_{hvac} at a humidity ratio of 0.018 kg/kg$_{da}$ and a temperature of 26 °C is 1.53 in the solar-assisted hybrid SDCS and 1.49 in the hybrid SDCS. The COP_{hvac} of systems at an outdoor temperature of 32 °C is approximately 18% lower than at 26 °C due to the temperature effect. At an outdoor temperature of 32 °C, the COP_{hvac} of the solar-assisted hybrid SDCS system is 7% greater than that of the hybrid SDCS. The maximum COP_{hvac} of the solar-assisted hybrid SDCS at an outdoor temperature of 32 °C is 1.369 for a humidity ratio of 0.0175 kg/kg$_{da}$, while the maximum COP_{hvac} of the hybrid SDCS is 1.218.

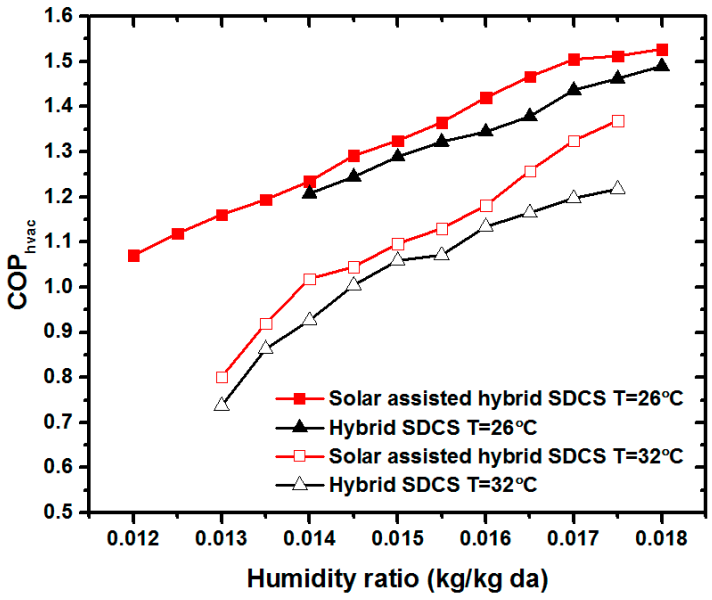

Figure 12. Comparison of COP_{hvac} at different outdoor humidity ratios.

4. Conclusions

In this study, a solar-assisted hybrid SDCS system was developed in which solar-heated water is used as a heat source for the regeneration process in addition to heat from the condenser of an integrated heat pump. A solar thermal collector sub-system is used to generate the solar regeneration water. Experiments were conducted in the typical hot and humid weather of Taichung, Taiwan, from the spring to fall seasons. According to the experiment results, several points can be concluded from the study, as follows:

(a) Solar-assisted hybrid SDCSs are feasible for use in hot and humid locations such as Taichung. Such systems can utilize solar energy as an additional heat source for the regeneration process. Therefore, the regeneration temperature of the system can be increased and the dehumidification effect can also be enhanced. Compared to the hybrid SDCS, the overall performance of the solar-assisted hybrid SDCS in terms of power consumption was found to be approximately 10% greater in the study. For a solar SDCS, a larger area and capacity of the solar thermal collector are required in high humidity environments.

(b) Higher humidity ratios lead to better *MRR* values for each solid desiccant cooling system configuration.

(c) The performance of a SDCS is very sensitive to changes in ambient conditions. The performance of each system configuration is better for higher outdoor humidity ratios. In terms of outdoor temperature, the COP_{hvac} of both systems increases with outdoor temperature. However, there are optimum values of the outdoor temperature for the COP_{hvac} of the system. When the ambient temperature is greater than the optimum value, the COP_{hvac} gradually decreases with the increase in ambient temperature. In this study, for the hybrid SDCS, the optimum outdoor temperature is between 26 and 27 °C, and for the solar-assisted hybrid SDCS, the optimum temperature range is 27–30 °C. Beyond these ranges, the overall performance of both systems will decline severely.

Author Contributions: Research concept were proposed by W.-J.L., D.F. and F.R.F.; data processing and the manuscript preparation were conducted by Y.-S.C., F.H.M. and U.N.A.; data analysis and interpretation were implemented by W.-J.L., D.F. and F.R.F.; manuscript editing was performed by W.-J.L., and F.H.M.

Funding: This research was funded by the Ministry of Science and Technology of Taiwan under grant number MOST 106-2221-E-167-026 and MOST 104-2221-E-167-026-MY2.

Conflicts of Interest: The authors declare no conflict of interest.

Nomenclature

A	area (m^2)	Q	heat capacity (kW)
COP	coefficient of performance	RH	relative humidity (%)
DCS	desiccant cooling system	rph	rotations per hour
E	power consumption (kW)	SDCS	solid desiccant cooling system
h	specific enthalpy (kJ/kg)	SF	solar fraction
I	solar irradiation (W/m^2)	SMR	specific moisture removal (kg/kg_{da})
$\dot{m}$	mass flow rate (kg/s)	T	temperature (°C)
MRR	moisture removal rate (kg/h)	Td	temperature declination (°C)
P	power (kW)	ω	humidity ratio (kg/kg_{da})

Subscripts

η	effectiveness	a	process air
c	cooling	ra	return air
soc	solar collector	reg	regeneration air
$hvac$	HVAC system	sa	supply air
lt	latent	sol	solar
m	month	tot	total
oa	outside air		

References

1. Wyon, D.P. The Effects of indoor air quality on performance and productivity. *Indoor Air* **2004**, *14*, 92–101. [CrossRef] [PubMed]
2. ANSI/ASHRAE Standard 55-2013. Available online: https://www.ashrae.org/technical-resources/bookstore/standard-55-thermal-environmental-conditions-for-human-occupancy (accessed on 15 May 2018).
3. Li, K.Y.; Luo, W.J.; Huang, J.Z.; Chan, Y.C.; Faridah, D. Operational Temperature Effect on Positioning Accuracy of a Single-Axial Moving Carrier. *Appl. Sci.* **2017**, *7*, 420. [CrossRef]
4. World Energy Outlook. Available online: https://www.iea.org/media/weowebsite/2008-1994/WEO2004.pdf (accessed on 15 May 2018).
5. Pérez-Lombard, L.; Ortiz, J.; Pout, C. A review on buildings energy consumption information. *Energy Build.* **2008**, *40*, 394–398. [CrossRef]
6. Inasawa, S.; Suzuki, R.; Qian, E.W.; Kitajima, T.; Yamashita, Y. Ozone layer depletion and its effects: A review. *Int. J. Environ. Sci. Dev.* **2011**, *2*, 30–37.
7. American Society of Heating, Refrigerating and Air Conditioning Engineers (ASHRAE). Desiccant dehumidification and pressure-drying equipment. In *2016 ASHRAE Handbook—Fundamentals (SI Edition)*; ASHRAE Inc.: Atlanta, GA, USA, 2016; p. 3.
8. Luo, W.J.; Kuo, H.C.; Wu, J.Y.; Faridah, D. Development and analysis of a new multi-function heat recovery split air conditioner with parallel refrigerant pipe. *Adv. Mech. Eng.* **2016**, *8*, 1–12. [CrossRef]
9. Mandegari, M.; Pahlavanzadeh, H. Introduction of a new definition for effectiveness of desiccant wheel. *Energy* **2009**, *34*, 797–803. [CrossRef]
10. Chang, C.C.; Luo, W.J.; Lu, C.W.; Cheng, Y.S.; Tsai, B.Y.; Lin, Z.H. Effects of process air conditions and switching cycle period on dehumidification performance of desiccant-coated heat exchangers. *Sci. Technol. Built Environ.* **2016**, *23*, 81–90. [CrossRef]
11. Narayanan, R.; Halawa, E.; Jain, S. Performance characteristic of solid-desiccant evaporative cooling system. *Energies* **2018**, *11*, 2574. [CrossRef]
12. Narayanan, R.; Halawa, E.; Jain, S. Dehumidification potential of a solid desiccant based evaporative cooling system with an enthalpy exchanger operating in subtropical and tropical climates. *Energies* **2019**, *12*, 2704. [CrossRef]
13. Guidara, Z.; Elleuch, M.; Bacha, H.B. New solid desiccant solar air conditioning unit in Tunisia: Design and simulation study. *Appl. Therm. Eng.* **2013**, *58*, 656–663. [CrossRef]
14. Enteria, N.; Yoshino, H.; Mochida, A.; Satake, A.; Yoshie, R.; Takaki, R.; Yonekura, H.; Mitamura, T.; Tanaka, Y. Performance of solar-desiccant cooling system with Silica-Gel (SiO_2) and Titanium Dioxide (TiO_2) desiccant wheel applied in East Asian climates. *Sol. Energy* **2012**, *86*, 1261–1279. [CrossRef]
15. Speerforck, A.; Ling, J.; Aute, V.; Radermacher, R.; Schmitz, G. Modeling and simulation of a desiccant assisted solar and geothermal air conditioning system. *Energy* **2017**, *141*, 2321–2336. [CrossRef]
16. White, S.D.; Kohlenbach, P.; Bongs, C. Indoor temperature variations resulting from solar desiccant cooling in a building without thermal backup. *Int. J. Refrig.* **2009**, *32*, 695–704. [CrossRef]
17. Jani, D.B.; Mishra, M.; Sahoo, P.K. Experimental investigation on solid desiccant–vapor compression hybrid air-conditioning system in hot and humid weather. *Appl. Therm. Eng.* **2016**, *104*, 556–564. [CrossRef]
18. Jani, D.B.; Mishra, M.; Sahoo, P.K. Performance analysis of a solid desiccant assisted hybrid space cooling system using TRNSYS. *J. Build. Eng.* **2018**, *19*, 26–35. [CrossRef]
19. Worek, W.M.; Moon, C.J. Simulation of an integrated hybrid desiccant vapor-compression cooling system. *Energy* **1986**, *11*, 1005–1021. [CrossRef]
20. Hwang, W.B.; Choi, S.; Lee, D.Y. In-depth analysis of the performance of hybrid desiccant cooling system incorporated with an electric heat pump. *Energy* **2017**, *118*, 324–332. [CrossRef]
21. Jani, D.B.; Mishra, M.; Sahoo, P.K. Performance studies of hybrid solid desiccant-vapor compression air-conditioning system for hot and humid climates. *Energy Build.* **2015**, *102*, 284–292. [CrossRef]
22. Merabti, L.; Merzouk, M.; Merzouk, N.K.; Taane, W. Performance study of solar driven solid desiccant cooling system under Algerian coastal climate. *Int. J. Hydrogen Energy* **2017**, *42*, 28997–29005. [CrossRef]
23. Beccali, M.; Finocchiaro, P.; Nocke, B. Energy performance evaluation of a demo solar desiccant cooling system with heat recovery for the regeneration of the adsorption material. *Renew. Energy* **2012**, *44*, 40–52. [CrossRef]

24. Beccali, M.; Finocchiaro, P.; Nocke, B. Energy and economic assessment of desiccant cooling systems coupled with single glazed air and hybrid PV/thermal solar collectors for applications in hot and humid climate. *Sol. Energy* **2009**, *83*, 1828–1846. [CrossRef]
25. Fong, K.F.; Chow, T.T.; Lee, C.K.; Lin, Z.; Chan, L.S. Solar hybrid cooling system for high-tech offices in subtropical climate: Radiant cooling by absorption refrigeration and desiccant dehumidification. *Energy Convers. Manag.* **2011**, *52*, 2883–2894. [CrossRef]
26. Fong, K.F.; Chow, T.T.; Lee, C.K.; Lin, Z.; Chan, L.S. Advancement of solar desiccant cooling system for building use in subtropical Hong Kong. *Energy Build.* **2010**, *42*, 2386–2399. [CrossRef]
27. Bareschino, P.; Pepe, F.; Roselli, C.; Sasso, M.; Tariello, F. Desiccant-Based Air Handling Unit Alternatively Equipped with Three Hygroscopic Materials and Driven by Solar Energy. *Energy* **2019**, *12*, 1543. [CrossRef]
28. Li, H.; Dai, Y.J.; Li, Y.; La, D.; Wang, R.Z. Case study of a two-stage rotary desiccant cooling/heating system driven by evacuated glass tube solar air collectors. *Energy Build.* **2012**, *47*, 107–112. [CrossRef]
29. Jani, D.B.; Mishra, M.; Sahoo, P.K. A critical review on application of solar energy as renewable regeneration heat source in solid desiccant-vapor compression hybrid cooling system. *J. Build. Eng.* **2018**, *18*, 107–124. [CrossRef]
30. Rambhad, K.S.; Walke, P.V.; Tidke, D.J. Solid desiccant dehumidification and regeneration methods: A review. *Renew. Sustain. Energy Rev.* **2016**, *59*, 73–83. [CrossRef]
31. Relative Humidity Table of Taiwan. Available online: https://www.cwb.gov.tw/V7e/climate/monthlyMean/tx.htm (accessed on 14 April 2018).